JOURNAL OF SOLID STATE CHEMISTRY 12, 177–185 (1975)

Oxide Optical Memories: Photochromism and Index Change*

D. L. STAEBLER

RCA Laboratories, Princeton, New Jersey 08540

Received July 3, 1974

Due to the many valence states available to transition element ions, transition element oxides doped with these impurities are particularly useful for optical storage. Either the color (as in $SrTiO_3$) or refractive index (as in $LiNbO_3$) of these materials can be changed by exposure to light. Color change (photochromism) involves optically induced oxidation–reduction effects that can also be produced by electrochromic treatments. Large index change occurs in electrooptic crystals, and is due to the optical generation of internal space charge fields. The latter process is highly useful for bulk hologram storage, particularly since the resulting holograms can be fixed by a simple heat treatment. The mechanisms and capabilities of these processes will be discussed with emphasis on photochromism and electrochromism in Ni,Mo doped $SrTiO_3$; and hologram storage in Fe doped $LiNbO_3$.

I. Introduction

Due to the many valence states available to transition element ions (*1*), transition element oxides doped with these impurities are particularly useful for optical storage. The storage arises from optical excitation of free carriers from the impurity sites, migration of the carriers to another site, and subsequent retrapping. Color change (photochromism) can occur when two different species of impurities are involved, and charge is transferred from one to the other. This leads to oxidation–reduction colorations that can also be achieved by chemical or electrical (i.e., electrochromic) means.

Large index changes can occur with only one species of impurity. Here, storage is associated with the net transport of charge from one part of the crystal to another. This sets up a space charge field that can strongly modulate the refractive index if the host material has a strong electrooptic effect. This process is highly useful for storage of volume holograms, particularly since the holograms can be made to be optically stable, i.e., they can be fixed.

This paper describes the present situation in the understanding and application of the above phenomena. Emphasis is placed on Ni,Mo doped $SrTiO_3$ (photochromism and electrochromism) and Fe doped $LiNbO_3$ (hologram storage, erasure, and fixing). Areas of future research are discussed.

II. Photochromism

Photochromic materials are those which reversibly change color from one state to another under exposure to light of different wavelengths (*2*). In comparison to photographic materials, photochromics have the advantage of simplicity (i.e., no processing) and the possibility of diffraction-limited resolution. They have, however, no mechanism for gain, as do photographic materials, and also are quite easily erased either thermally or upon exposure to light. The capability for erasure can be an advantage or a limitation, depending on the application. For example, those materials are clearly not suitable for applications that require nondestructive readout, but in principle, can be used in systems in which the recording material is to be used over and over again.

* Invited paper.

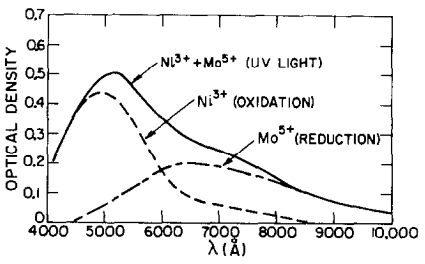

FIG. 1. Absorption bands produced in a 0.25 mm thick sample of $SrTiO_3$:Ni,Mo measured at 77°K. The broadened band edge absorption (*4*) that leads to the photochromic process pictured in Fig. 2 has been subtracted out.

Photochromism has been observed in many oxide materials (*2*), including glass, sodalite, apatite, TiO_2, $CaTiO_3$, and $SrTiO_3$. The $SrTiO_3$ materials will be discussed here. They perform as well as or better than the others, and have been investigated quite thoroughly by EPR and optical techniques (*2–4*). $SrTiO_3$ photochromics are made by doping with two different transition elements. Ni,Mo and Fe,Mo are two sets that work particularly well. The following discussion on the Ni,Mo doped crystals apply equally well to Fe,Mo doped crystals, with Fe playing the same role as the Ni. The impurities are introduced during growth, in concentrations of ~0.01–0.5% by weight of oxide, and substitutionally occupy Ti sites.

The various absorption spectra that can be induced in Ni,Mo doped $SrTiO_3$ by various means are shown in Fig. 1. Upon reduction (heating in an oxygen-free atmosphere), a crystal takes on a blue hue due to the absorption spectrum characteristic of Mo^{5+} ions. The Ni ions are in the Ni^{2+} state and do not contribute appreciably to the absorption. Upon oxidation (heating in an oxygen atmosphere), both ions increase their valence state. As a result, the crystal becomes brown due to absorption spectrum of Ni^{3+} ions. The Mo are converted to the Mo^{6+} state in which they do not strongly absorb light. Finally, there is an intermediate clear state that can be obtained by partial reduction, in which only Ni^{2+} and Mo^{6+} are present in the crystal. It is in this state that the photochromic effect is most dramatic. Exposure to uv light (~3800–4500 Å) generates both Ni^{3+} and Mo^{5+} ions, resulting in a broad absorption throughout the visible portion of the spectrum. This coloration remains for several minutes after the light is turned off, but it can be quickly bleached by exposure to visible light.

The above photochromic process arises from a photoreversible transport of charge between impurity ions. This can be described schematically as

$$Ni^{2+} + Mo^{6+} \xrightarrow{uv} Ni^{3+} + Mo^{5+}.$$

Three possible ways in which this can occur are shown in Fig. 2. Although the nature of the charge carrier is not known, photoconductivity experiments (*5*) have definitely established that some form of free carrier transport is involved in the process.

Table I shows the important parameters for practical application of these materials. The sensitivity is fair, only about 30 times lower than one could expect in a perfect photochromic. A perfect material is one in which each incident photon creates an absorption center with unity oscillator strength.

For $SrTiO_3$, only part of the decrease in sensitivity can be accounted for by a lower

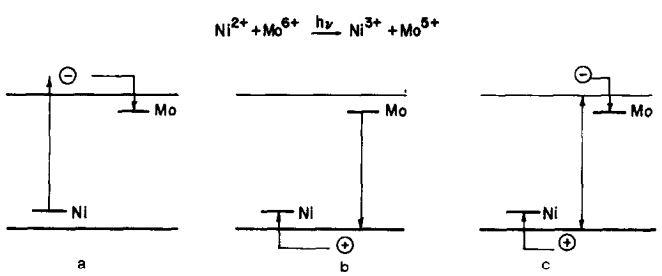

FIG. 2. Schematic diagram of possible charge-transfer mechanisms responsible for the uv coloration shown in Fig. 1a: electron excitation; b: hole excitation; c: electron–hole pair excitation.

TABLE I

$SrTiO_3$ PHOTOCHROMIC MATERIAL

Dopants	Color[a] (mJ/cm²)	Bleach[b] (mJ/cm²)	Max α[c] (cm^{-1})	300°K Decay (min)
Ni, Mo	30	300	70	2–10
Fe, Mo	30	60	70	1–5

[a] 3800–4500 Å.
[b] 4600–9000 Å.
[c] At 5000 Å.

oscillator strength ($f \sim 0.2$ for Mo^{5+} and Ni^{3+}). The rest must be due to a low (~10%) quantum efficiency for charge transfer. The thermal stability of the uv coloration is also fair, lasting long enough to easily read out the recorded information, but not long enough to consider this as a permanent record. Since in some computer applications the information can be periodically updated, this lack of permanancy should not be considered as a fundamental limitation.

A basic problem with these materials is their relatively low coloration strengths. To obtain a significant effect, i.e., 50% absorption change, a crystal thicker than ~0.25 mm must be used. With this thickness, one cannot easily take advantage of the essentially grain free resolution capabilities of the material. In principle, the resolution is limited only by optical diffraction. That is, it depends on the smallest possible cross section of a focused light beam. For a thick crystal, the effective spot size is larger because a spot focused on the front of the crystal is out of focus at the back. Very heavily doped crystals have been studied in an attempt to reduce the thickness, but in these the coloration decays quite rapidly. This is thought to be due to tunneling between impurity sites (*2*). One approach for high resolution storage is to record volume holograms (*6*, *7*). Absorption effects, however, are not well suited to this technique (*8*); the large index changes discussed in Section IV are much better.

At present, inorganic photochromic materials can be used in situations where relatively long optical path lengths can be tolerated. A well-known application is for sunlight activated sunglasses. Another application is in the possible control of light passing through an optical waveguide (*9*), the basic component in the quite active field of integrated optics.

III. Electrochromism

Although not strictly an optical storage technique, electrochromism fits well into this discussion, particularly since a striking example of this effect occurs in the $SrTiO_3$ photochromic materials described in Section II. Electrochromism is the reversible coloration of a material under the application of an electric field. Figure 3 shows a crystal of Ni,Mo doped $SrTiO_3$ colored by this method. It was done by heating the crystal to ~250°C, and applying ~100 V to two tungsten probes pressed against the face of the sample. The color forms within a few minutes. It occurs more quickly if either the temperature or voltage is increased.

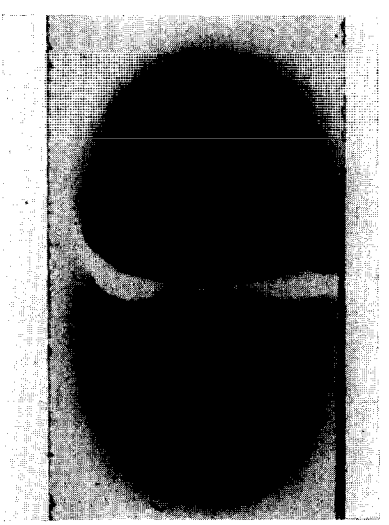

FIG. 3. A crystal of $SrTiO_3$:Ni,Mo colored by the electrochromic process described in the text. The left side is blue (reduced,) the right side brown (oxidized). The point electrodes (+ right, – left) were on the same side of the crystal, and were situated close to the outer edge of the colored regions. The clear stripe in the middle was produced by briefly reversing the voltage.

The mechanism for this process in $SrTiO_3$ has been identified by optical and electronic analysis (*10*). It is initiated by thermally activated oxygen vacancies drifting in the applied field. Charge compensation by hole injection (at the anode) and electron injection (at the cathode) allows two regions of color to form. A blue color (Mo^{5+}) due to reduction forms at the cathode, a brown color (Ni^{3+}) due to oxidation forms at the anode. The two spectra are shown in Fig. 1. An important point is that the two colored regions have higher conductivity than the clear crystal; i.e., they serve as extensions of the electrodes. Thus they can grow, propagate into the crystal toward each other, and meet somewhere in between the two contacts. Upon subsequent reversal of the voltage, a sharp boundary forms between the two regions (see Fig. 3), and then the colors recede. Ultimately they disappear at the contacts, reappear at the opposite contacts, and then grow as before.

The advantages of this effect are high coloration and good stability. Absorption coefficients approaching 10^4 cm^{-1} have been achieved in these crystals, more than two orders of magnitude higher than that recorded by the photochromic process. At the same time, the electrochromic colorations are quite stable, particularly at room temperature. Some crystals have remained colored for years with no evidence of decay. The disadvantages are the need for creating an electric field pattern to record detailed information, (although this could be done optically with a photoconductor–electrochromic sandwich), and the need (in $SrTiO_3$) of a elevated temperature to mobilize the ionic defects responsible for the coloration effect. A material with high ionic conductivity at lower temperature is preferred. Deposited thin films of WO_3 have shown quite promising effects at room temperature (*11*, *12*).

The maximum sensitivity for an electrochromic process can be easily calculated. If one assumes that each injected charge leads to one absorption center having a ~1 eV wide band of unity oscillator strength, then a significant coloration in a 1 cm^2 area requires a total of $\sim 10^{-2}$ C. If this is to occur in 1 sec, the average current required is only 10 mA.

IV. Index Change

Optically induced index changes occur in many electrooptic and ferroelectric oxides. Some of them are $LiNbO_3$ (*13*), $(SrBa)Nb_2O_6$ (*14*), $LiTaO_3$ (*15*), $BaTiO_3$ (*16*), and $Ba_2NaNb_5O_{15}$ (*17*). The effects that occur in Fe doped $LiNbO_3$ are discussed in the following. This material is fairly well understood, and has a wide range of possible applications for both read/write and read/only systems.

The role of Fe impurities in $LiNbO_3$ is to provide a set of partially occupied, photoionizable electron traps (*18*, *19*). The trap when empty is the Fe^{3+} ion, and when occupied is the Fe^{2+} ion. The latter has a strong absorption band due to the transfer of an electron to the conduction band (*20*). Figure 4 shows this absorption. It is produced by annealing the crystal in an argon atmosphere or in Li_2CO_3 powder (*21*). Upon oxidation, the Fe are converted to the Fe^{3+} state which has no absorption. The corresponding changes in trapped electron density must be charge compensated by other defects, oxygen vacancies perhaps, but these apparently are not directly involved in the storage process.

Index changes occur in this material when the trapped electrons are moved from one part of the crystal to another. Figure 5 shows

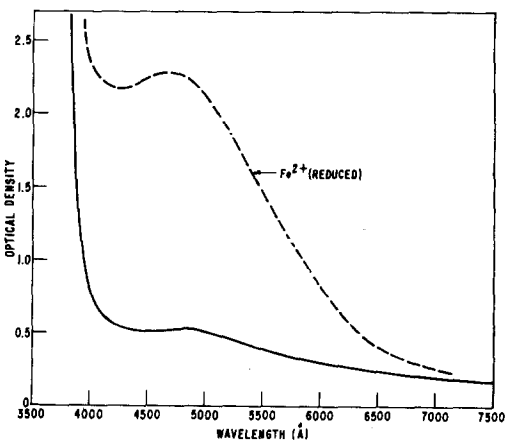

FIG. 4. Fe^{2+} absorption produced by reduction in a 2 mm thick sample of 0.05% Fe doped $LiBbO_3$. The absorption strength corresponds to $\sim 3 \times 10^{18}$ Fe^{2+} ions/cm^3 (*21*).

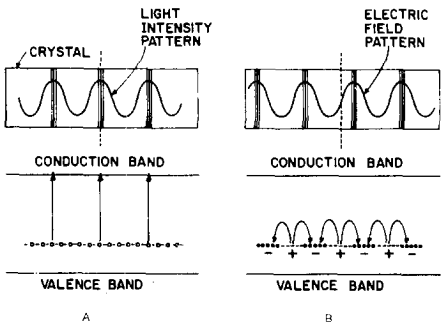

FIG. 5. Pictorial representation of index change produced by (a) selective photoexcitation of deep traps and (b) redistribution of the electrons. The solid lines running through the crystal represent that this occurs in the bulk.

how this occurs during storage of a simple hologram, i.e., a sinusoidal diffraction grating. Before storage, the trapped electrons are distributed uniformly throughout the crystal. When the crystal is then exposed to a sinusoidal light pattern (such as that formed by two plane coherent light beams), absorption by the trapped electrons produces a corresponding pattern of free carriers in the conduction band. The electrons then migrate due to either (1) drift in a uniform electric field (*13*, *22*) or (2) diffusion caused by periodic gradients in the free carrier density (*22*, *23*). The latter occurs in crystals that contain a relatively low concentration ($<10^{17}$ cm^{-3}) of Fe^{3+} ions (*24*). In successive steps of excitation, migration, and retrapping, the electrons are rearranged to produce regions of uncompensated space charge. Figure 4 shows an extreme case. Nearly all the trapped charge are displaced from the regions of high light intensity into regions of low light intensity. The resulting space charge sets up a periodic electric field pattern that modulates the refractive index via the electrooptic effect. This gives a phase hologram.

To record and read out these holograms, one typically uses the setup shown in Fig. 5. The crystal is placed at the intersection of two laser beams, a uniform reference beam, and an object beam that in storage applications contains information in the form of intensity variations over its cross section. In the studies discussed here, however, both beams are uniform. For storage, both beams are used to produce the simple interference pattern pictured in Fig. 4. To read out the resulting hologram, only the reference beam is used. The hologram diffracts this beam to perfectly reconstruct the object beam. The diffraction efficiency of the hologram is determined by measuring the intensity of the diffracted beam and comparing it to that of the reference beam. Diffraction efficiencies more than 50% can be easily achieved in some crystals, and theory shows that this corresponds to a space change density of only $\sim 10^{16}$ cm^{-3} in a $\sim$1 mm thick crystal of $LiNbO_3$.

A. Erasure

A very significant feature of this storage technique is that the pattern can be erased with light of the same wavelength used for storage. This is done by exposing the crystal to a light beam, the reference beam for example, that uniformly excites all trapped electrons. This allows the electrons to uniformly redistribute, and thus erases the hologram. It has been shown (*22*, *24*) that the erasure process can be described as drift of the electrons in the space charge field of the hologram, i.e., dielectric relaxation. It is an exponential process with a time constant given by ε/σ, the dielectric constant divided by the photoconductivity.

The erasure sensitivity of these materials can be drastically enhanced by reduction treatments (*24*). The purpose of the treatments is to convert most of the ions into the divalent state leaving few empty traps (Fe^{3+} ions). This increases the free carrier lifetime, and thus increases the photoconductivity per absorbed photon. Figure 6 shows this effect for three $\sim$2 mm thick crystals of

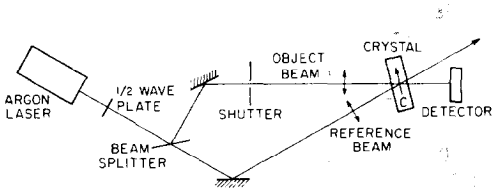

FIG. 6. Typical apparatus for recording (both beams) and reading (reference beam only) holograms in an electrooptic crystal. The *c* axis and polarization vectors are aligned for maximum index modulation.

0.0025% Fe doped $LiNbO_3$ reduced to progressively greater degrees (*21*). The optical absorption at 4880 Å was ~0.3 O.D. for each one, corresponding to an Fe^{2+} concentration of $\sim 5 \times 10^{17}$ cm^{-3}. The Fe^{3+} concentration ranges from $<10^{17}$ cm^{-3} for the upper one to $<7 \times 10^{15}$ cm^{-3} for the lower one. The maximum efficiency that can be obtained (the beginning point of the lines in Fig. 6) also decreases upon reduction. This is probably because the low Fe^{3+} concentration in these crystals limits the maximum space charge that can be built up (*24*).

Table II shows the energy required for storage and erasure of holograms in these crystals. Also shown for comparison is a crystal with a high concentration of Fe^{3+} ions ($\sim 10^{19}$ cm^{-3}). This is a ~0.053% Fe doped sample that was lightly reduced (~10%) to get an Fe^{2+} concentration similar to the others. One can record very high diffraction efficiencies in this crystal, but they are extremely hard to erase. This can be quite important for multiple storage purposes as will be discussed later in this paper.

Compared to the photochromic crystals of Table I, Fe doped $LiNbO_3$ has the advantage of higher thermal stability and ease of erasure. The good stability is due to the high activation energy (*20*, *25*) (~1.4 eV) of the Fe traps. The sensitivity is comparable to the photochromics, but in principle could be increased by many orders of magnitude. The maximum possible sensitivity of the process occurs when each incident photon moves an electron by a distance roughly equal to the period of the sinusoidal pattern (*22*, *26*). For $LiNbO_3$, this means that only $\sim 10^{-4}$ J/cm² of 4880 Å light would be required to record and erase a ~1% hologram. Apparently, the sensitivity of this material at present is being limited by small mean free carrier ranges, a conclusion consistent with the effect of electric fields on the storage behavior of the crystals (*24*, *26*). This situation could be improved by extreme degrees of reduction, but at the expense of a drastic decrease in diffraction efficiency. One solution would be to use, instead of Fe, a different set of traps with much lower capture cross section. This would increase the mean range without limiting the efficiency. Research in this area may prove fruitful. Host materials with higher electrooptic coefficients than for $LiNbO_3$ have shown high sensitivity (*27*), but it should be kept in mind that such materials generally have a higher dielectric constant and this increases the amount of space charge needed to get a given field strength. The important factor is the ratio of the electrooptic coefficient to the dielectric constant, and this shows little variation from material to material (*28*). Improved storage sensitivity in Fe doped $LiNbO_3$ has been recently reported (*29*), but the origin of the improvement is not certain.

TABLE II

$LiNbO_3$:Fe

Fe Reduction[a] (%)	Readout efficiency (%)	Storage[b] (mJ/cm²)	Erase[b] (mJ/cm²)	300°K Decay
10	40	1000	6000	>1 mo
>80	1	100	100	>1 mo
>94	0.6	30	30	—
>98.5	0.08	12	12	—

[a] Estimated from EPR and optical measurements.
[b] At 4880 Å.

B. Fixing

Hologram fixing is accomplished in $LiNbO_3$ by heating the crystal during or after storage (*30*). At temperatures above ~100°C, $LiNbO_3$ has an ionic conductivity that quickly neutralizes the space charge patterns of the hologram (*31*). Since the electrons are so deeply trapped that they remain stable during this process, the result is an ionic charge pattern that perfectly mirrors the patterns of the recorded hologram. Upon cooling to room temperature, the ionic pattern is frozen in. The crystal is then exposed to light which tends to redistribute the electrons. The resulting space charge field is due to the ionic pattern and hence does not decay upon readout.

Figure 7 schematically shows what happens to the diffraction efficiency during the above steps. The optical erasure of a normal hologram is shown for comparison. The fixing

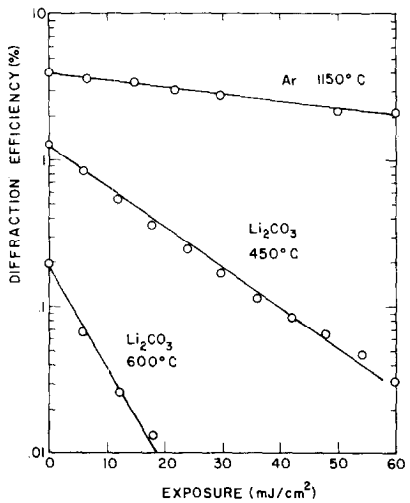

FIG. 7. Diffraction efficiency during erasure for crystals with three different conversions of Fe to Fe^{2+}. The Fe^{3+} concentration of the crystals should be inversely proportional to the shape of the lines (*24*).

process also leads to decay of the diffraction efficiency, but does not erase the pattern. It neutralizes the space charge field, and thus removes the index modulation. That erasure has not occurred is graphically shown by the reappearance of the hologram upon redistribution of the electrons. The final diffraction efficiency can be reduced by electronic screening effects (*31*), but this is not a severe problem.

Heating the crystal to a higher temperature than that used for fixing will erase the fixed hologram, after which the crystal can be used again. The erasure is due to thermal excitation of the trapped electrons. The electrons then redistribute uniformly, followed by the ions as they attempt to maintain charge neutrality. The result is erasure of both patterns, ionic and electronic. The same can occur if the sample is exposed to light at the temperature used for fixing.

Figure 8 shows the thermal erasure and fixing times as a function of temperature for a ~0.001% Fe doped sample. The erasure activation energy is ~1.4 eV, the activation energy of the Fe^{2+} ions (*20*, *25*). The fixing activation energy is ~1.1 eV. The ionic species responsible for this process has not been identified. It appears in all crystals, regardless of doping (*31*).

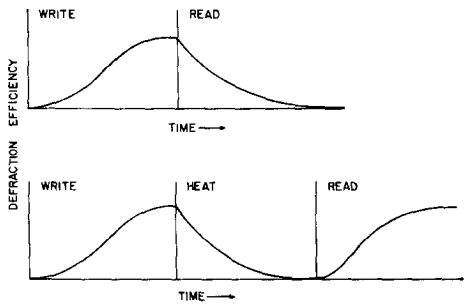

FIG. 8. Diffraction efficiency upon readout of a normal hologram (top) and a hologram fixed by the thermal process discussed in the text (bottom).

Hologram fixing is extremely useful for applications that require long term archival storage, i.e., read only applications. Some holograms have shown no degradation, in either diffraction efficiency or quality of readout image, after nearly two years of continuous use. In addition, hologram fixing allows one to take full advantage of the multiple storage capacity of thick holograms (*32*).

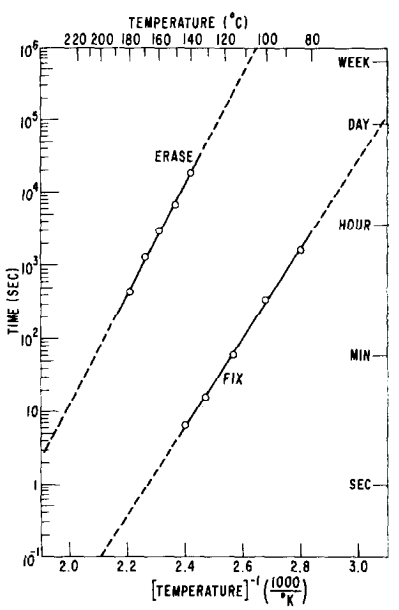

FIG. 9. Time constants for thermal fixing and erasing of holograms in a 0.001% Fe doped sample of $LiNbO_3$. The *lower* line corresponds to the thermal decay shown in Fig. 8.

A thick hologram, i.e., one whose thickness is much greater than the periodicity of its pattern, has an angular selectivity for readout in a manner analogous to Bragg diffraction of X rays. When a crystal is rotated slightly, the readout of one hologram disappears, and another one recorded at that new angle can be seen. In this manner, more than 10^3 holograms can be, in principle, stored in a 1 cm thick crystal (*33*). The resolution of each hologram is diffraction limited, providing the capability of storing more than 10^{11} bits in a centimeter cube of material. The point of fixing the holograms is that each one is stored throughout the entire bulk of the crystal, only their angle is different. If they are fixed, then one of them can be read out without erasing the others.

Recent results (*34*) have shown that the best approach for storing multiple fixed holograms in Fe doped $LiNbO_3$ is to use moderately doped crystals, like the top one in Table II, which have been lightly reduced to keep the Fe^{2+} absorption at an acceptable level. The crystal is heated to an elevated temperature (~160°C), and then the holograms are sequentially recorded, one after the other at different angles. The crystal is not cooled until all the holograms are recorded. The sensitivity of process (~10–20 J/cm^2 for a ~40% diffraction efficiency fixed hologram) is less than for more lightly doped crystals (*30*), but this is more than compensated by its simplicity and good storage capacity. More then 100 holograms have been recorded thus far, with ~0.5% diffraction efficiency, and better results are expected. The good capacity of these crystals is a result of their low erasure sensitivity, in comparison to their sensitivity for storage. The origin of this write/erase asymmetry at elevated temperatures is not well understood. There is evidence that it arises from an apparent internal field that becomes significant in $LiNbO_3$ when a sufficient concentration of Fe^{3+} ions is present (*24*, *34*).

V. Conclusion

Charge transport phenomena in impurity doped transition element oxides can be used for a variety of optical storage applications. The storage arises from optically initiated oxidation or reduction of the impurities. Both absorption change (photochromism) and index change (phase hologram storage) occur. Optical erasure, reversibility, and high resolution are important features of these materials. High optical stability can also be achieved by judicious use of thermally activated ionic transport. Examples of the latter are electrochromism in $SrTiO_3$ and hologram fixing in $LiNbO_3$. In addition to optical storage, these processes can also be used to study charge transport (both electronic and ionic) and localized electron traps in a variety of oxide materials.

Phase hologram storage is superior to photochromism for many applications, but the latter is still quite important. For example, photochromic effects have been recently used to optically control the hologram storage sensitivity of $LiNbO_3$ (*25*). This field is by no means exhausted, and future research should lead to significant advances in the understanding and application of these materials.

References

1. D. S. McClure, "Electronic Spectra of Molecules and Ions in Crystals," p. 127. Academic Press, New York, 1959.
2. B. W. Faughnan, D. L. Staebler, and Z. J. Kiss, *In* "Applied Solid State Science," Volume II, (R. Wolfe, Ed.), p. 107. Academic Press, New York, 1971.
3. B. W. Faughnan and Z. J. Kiss, *IEEE J. Quant. Electron.* **QE-5**, 17 (1969).
4. B. W. Faughnan, *Phys. Rev.* **4**, 3623 (1971).
5. R. Williams, *J. Appl. Phys.* **42**, 1131 (1971).
6. D. R. Bosomworth and H. J. Gerritsen, *J. Appl. Opt.* 7, 95 (1968).
7. J. Amodei and D. R. Bosomworth, *J. Appl. Opt.* **8**, 2473 (1969).
8. R. J. Collier, C. B. Burkhardt, and L. H. Lin, "Optical Holography." Academic Press, New York, 1971.
9. J. D. Crow, N. F. Borrelli, and T. P. Seward III, *Eighth International Quantum Electronics Conference, San Francisco*, June 10, 1974.
10. J. Blanc and D. L. Staebler, *Phys. Rev.* **B4**, 3548 (1971).
11. S. K. Deb, *Phil. Mag.* **27**, 801 (1973).
12. B. W. Faughnan, to be published.
13. F. S. Chen, J. T. LaMacchia, and D. B. Fraser, *Appl. Phys. Letters* **13**, 223 (1968).

14. J. B. THAXTER, *Appl. Phys. Letters* **15**, 210 (1969).
15. F. S. CHEN, *J. Appl. Phys.* **40**, 3389 (1969).
16. R. L. TOWNSEND AND J. T. LAMACCHIA, *J. Appl. Phys.* **41**, 5188 (1971); F. MICHERON AND G. BISMUTH, *Appl. Phys. Letters* **20**, 79 (1972).
17. J. J. AMODEI, D. L. STAEBLER, AND A. W. STEPHENS, *Appl. Phys. Letters* **18**, 507 (1971).
18. J. J. AMODEI, W. PHILLIPS, AND D. L. STAEBLER, *IEEE J. Quant. Elect.* **QE-7**, 63 (1971).
19. G. E. PETERSON, A. M. GLASS, AND T. J. NEGRAN, *Appl. Phys. Letters* **19**, 130 (1971).
20. M. G. CLARK, F. J. DISALVO, A. M. GLASS, AND G. E. PETERSON, *J. Chem. Phys.* **59**, 6209 (1974).
21. W. PHILLIPS AND D. L. STAEBLER, *J. Elect. Mat.* **3**, 601 (1974).
22. J. J. AMODEI, *RCA Rev.* **32**, 185 (1971).
23. D. L. STAEBLER AND J. J. AMODEI, *J. Appl. Phys.* **43**, 1042 (1972).
24. D. L. STAEBLER AND W. PHILLIPS, *Appl. Opt.* **13**, 788 (1973).
25. D. L. STAEBLER AND W. PHILLIPS, *Appl. Phys. Letters* **24**, 268 (1974).
26. L. YOUNG, W. K. Y. WONG, M. L. W. THEWALT, AND W. D. CORNISH, *Appl. Phys. Letters* **24**, 264 (1974).
27. J. B. THAXTER AND M. KESTIGIAN, *Appl. Opt.* **13**, 913 (1974).
28. A. MILLER, A. G. KASIPEDES, AND J. M. PELTZ, *Appl. Opt.* **10**, 1925 (1971).
29. PRADEEP SHAH, T. A. RABSON, F. K. TITTEL, AND T. K. GAYLORD, *Appl. Phys. Letters* **24**, 130 (1974).
30. J. J. AMODEI AND D. L. STAEBLER, *Appl. Phys. Letters* **18**, 549 (1971).
31. D. L. STAEBLER AND J. J. AMODEI, *Ferroelectrics* **3**, 107 (1972).
32. P. J. VAN HEERDEN, *Appl. Opt.* **2**, 393 (1963).
33. D. L. STAEBLER, to be published in Photographic Science and Engineering.
34. D. L. STAEBLER, W. BURKE, W. PHILLIPS, AND J. J. AMODEI, to be published.